View metadata, citation and similar papers at core.ac.uk
brought to you by CORE
provided by Scientific Open-access Literature Archive and Repository

IL NUOVO CIMENTO Vol. 34 C, N. 1 Gennaio-Febbraio 2011
DOI 10.1393/ncc/i2011-10809-x

Colloquia: IFA 2010

Proton imaging apparatus for protontherapy application

V. Sipala(1)(2)(*), M. Brianzi(3), M. Bruzzi(3)(4), M. Bucciolini(3)(5), G. A. P. Cirrone(6), C. Civinini(3), G. Cuttone(6), D. Lo Presti(1)(2), N. Randazzo(2), M. Scaringella(3)(4), C. Stancampiano(2), C. Talamonti(3)(4) and M. Tesi(4)

(1) *Dipartimento di Fisica, Università di Catania - via S. Sofia 64, I-95123 Catania, Italy*
(2) *INFN, Sezione di Catania - via S. Sofia 64, I-95123 Catania, Italy*
(3) *INFN, Sezione di Firenze - via G. Sansone 1, I-50019 Sesto Fiorentino (FI), Italy*
(4) *Dipartimento di Energetica, Università di Firenze - via S. Marta 3, I-50139 Firenze, Italy*
(5) *Dipartimento di Fisiopatologia Clinica, Università di Firenze - v.le Morgagni 85 I-50134 Firenze, Italy*
(6) *INFN, Laboratori Nazionali del Sud - via S. Sofia 62, I-95123 Catania, Italy*

(ricevuto il 7 Luglio 2010; approvato il 31 Luglio 2010; pubblicato online il 15 Febbraio 2011)

Summary. — Radiotherapy with protons, due to the physical properties of these particles, offers several advantages for cancer therapy as compared to the traditional radiotherapy with photons. In the clinical use of proton beams, a pCT (proton Computed Tomography) apparatus can contribute to improve the accuracy of the patient positioning and dose distribution calculation. In this paper a pCT apparatus built by the PRIMA (PRoton IMAging) Italian Collaboration will be presented and the preliminary results will be discussed.

PACS 29.40.Vj – Calorimeters.
PACS 87.57.Q- – Computed tomography.
PACS 29.40.-n – Radiation detectors.
PACS 07.05.Hd – Data acquisition: hardware and software.

1. – Introduction

The interest in the use of hadrons for the treatment of cancer results in a growing number of new projects in this area [1-3]. The main advantage in the use of these particles is a better conformation of dose to the target volume, linked to how these particles interact with matter. However, the accuracy of the proton therapy is currently limited by the uncertainty with which one knows the distribution of mass stopping powers of these particles in matter, which is determined, for each patient to be treated, from the distribution of the absorption coefficients of photons measured with CT [4]. The uncertainty could be reduced by measuring directly the mass stopping power with beam of proton through the use of a computerized axial tomography system with protons (pCT) [5].

(*) E-mail: valeria.sipala@ct.infn.it

© Società Italiana di Fisica

For this reason, the PRIMA (Proton IMAging) Collaboration [6] has designed and built an apparatus able to acquire tomographic images and to measure the mass stopping power distribution, using proton beams. The use of the pCT apparatus is foreseen in the pre-treatment phase, *i.e.* it is useful for the planning of the treatment, besides for the verification of the patient positioning during the first session.

The problem in using proton beams for imaging is that these particles do not have straight trajectories in the matter because of multiple Coulomb scattering. The "single tracking technique" whose principle is to track each single proton and to measure its residual energy is a promising method to overcome this difficulty [7, 8]. The first step towards developing a pCT apparatus is building a proton Computed Radiography (pCR) device, able to measure a single projection. Adding a rotating system in order to acquire multiple projections the pCT apparatus construction will be possible.

Supported by the MIUR and INFN, a pCR system has been designed and built [9-12], with field of view about $5 \times 5\,\mathrm{cm}^2$, consisting of a silicon tracker and a YAG:Ce crystal calorimeter. The aim is to detect protons with kinetic energy high enough to cross a human torso (250–270 MeV) with a rate of $\sim 1\,\mathrm{MHz}$ and to collect data with times of the order of the second, which satisfies the clinical requirements. The parameters to be measured are entrance and exit angles, positions and proton residual energy. These data are necessary to determine the most likely path (MLP) for the creation of a map of electronic densities of the tissue [13]. The radiography reconstruction algorithm has been already tested with pre-existing data [14]. In the future plans there is the development of adequate tomographic reconstruction algorithms and the validation of the developed algorithms on real data obtained with the pCR system rotating the phantom.

2. – pCR apparatus architecture

The pCR apparatus consists of a silicon tracker to sample the particle trajectory and a calorimeter to measure its residual energy. As shown in fig. 1, the tracker is composed of four x-y modules to measure the proton coordinates in the plane orthogonal to the beam line and a YAG:Ce scintillating crystal employed as calorimeter. Each tracker module communicates with the control terminal (PC) via an Ethernet (IEEE 802.3) connection. The calorimeter outputs are used in order to generate the trigger signal, necessary to the tracker as acquisition start, and the global event number (GEN), attached to all the data (calorimeter and the tracker) in order to allow an easy and unambiguous event building.

Each x-y tracker plane is composed of two identical tracker modules rotated by 90° one with respect to the other. The module includes a 256 channels single-side silicon microstrip detector, 8 VLSI (Very Large Scale Integrated) front-end chips and a FPGA-based digital electronics for data acquisition and transmission. The front-end chip includes 32 channels with a charge sensitive amplifier, a shaper and a comparator with external threshold. When a particle crosses the detector the electronic front-end gives a digital output. Moreover, by the Time Over Threshold (TOT) technique, the energy loss in the silicon microstrip detector can be reconstructed by digital output. The data are memorized in a RAM and sent off-line to the PC. The RAM chosen is able to acquire about 500000 events necessary for a clinical image.

The calorimeter is made of four YAG:Ce optically separated crystals, with size $3 \times 3 \times 10\,\mathrm{cm}^3$, arranged as a 2×2 matrix, produced by Crytur [15]. This material has been selected due to its short decay time (70 ns) and because its scintillation light is in the photodiode sensitivity range. The photodiode used is S3204 made by Hamamatsu [16]. A requirement of the system is the acquisition data rate which must reach

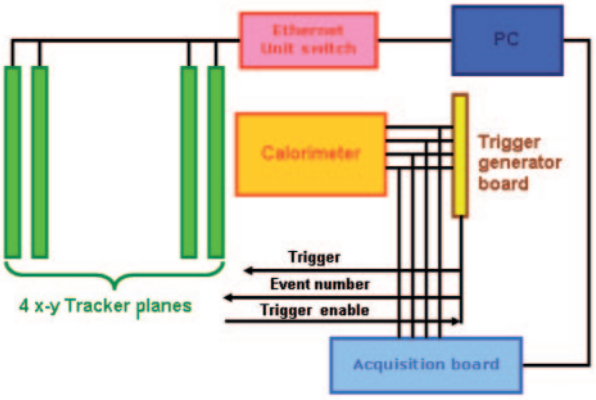

Fig. 1. – Schema of the pCR apparatus. It consists of 4 x-y tracker planes, a calorimeter, a trigger generator board, a commercial acquisition board. Tracker data are transferred by Ethernet connection to the PC.

1 MHz. For this reason, the calorimeter has been sectioned into four parts, so each crystal must be able to acquire at 250 kHz. The photodiode outputs are processed by a charge sensitive amplifier with "cold discharge" method [17] and a commercial hybrid shaper. Four signals are sampled in parallel mode by UF2-4032 acquisition commercial board [18].

3. – pCR apparatus status

The pCR apparatus has been completed. Each x-y plane has been tested separately with β-source. About the calorimeter, different tests were performed at Laboratori Nazionali del Sud (LNS) in the CATANA facility (proton energy up to 60 MeV) [19] and Loma Linda University Medical Center (LLUMC) (proton energy up to 200 MeV) in order to measure the resolution and the homogeneity of the crystal, the acquisition performance at high rate. An x-y plane has been coupled to the calorimeter and tested with 60 MeV proton beam at LNS.

Finally, all planes have been assembled with the calorimeter in the final configuration and in fig. 2 a picture of the apparatus placed along the beam line is shown. The test has been performed in the 1–10 kHz acquisition rate range.

Data taken during this recent test is currently under analysis. Several radiographies of an experimental phantom have been taken to measure the system resolution.

4. – Preliminary experimental results

Several tests have been carried out to understand the electrical performances of the front-end (by injecting a test pulse inside ASIC test inputs) and particle detection capabilities (with β-source and whit 60 MeV proton beam). Different output DC levels for channel outputs have been observed, so a fine threshold regulation on chip-by-chip basis through potentiometers has been implemented. In this configuration all the chips work in optimal conditions even with higher proton beam energy. In fig. 3, pulse duration, measured at 60 MeV proton beam and with 200 mV threshold voltage value over

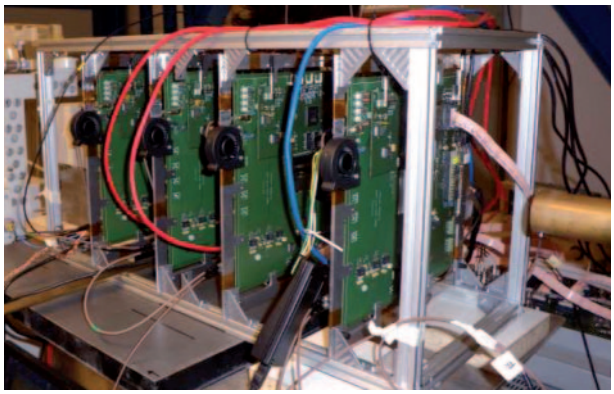

Fig. 2. – The picture of the pCR apparatus realized, positioned along the CATANA beam line.

the DC level, is plotted *versus* particles kinetic energy. Both the tracker modules exhibit the same slope but different intercept. This plot confirms the different chip DC voltage.

The tracker detection efficiency as a function of the threshold voltage has been measured using the 60 MeV proton beam: the efficiency remains at its maximum value ($\sim 98\%$) for about 150 mV above the noise limit. Using β-source, the threshold voltage value interval whit high efficiency is about 10 mV. However, according to Monte Carlo simulation, the charge released in the detector by β-source is equal to $1.5 \cdot 10^4$ electrons while the 250 MeV proton beam is about $3 \cdot 10^4$ electrons. So, these results ensure that our system is able to detect protons from a radiotherapy beam with good efficiency, because it will always have better performances than those we can measure with β-source.

Figure 4 shows the histogram of the charge released in the silicon strip from 60 MeV proton beam obtained using the TOT technique and the calibration curve of the single

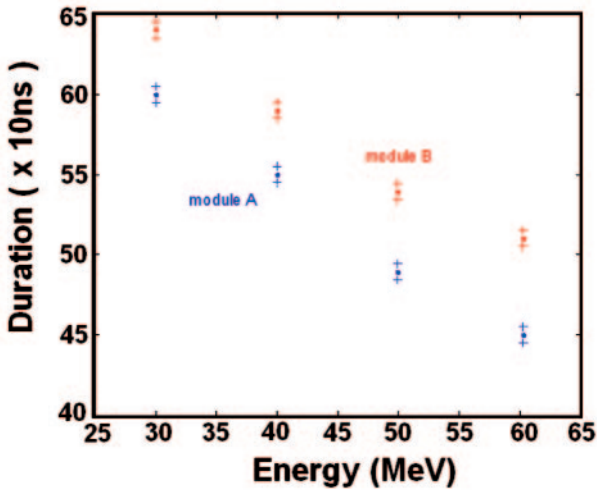

Fig. 3. – Most probable value of pulse duration T *vs.* proton kinetic energy E at fixed threshold ($\Delta V_{\text{th}} = 200$ mV). Duration is expressed in terms of clock cycles (clock period is 10 ns).

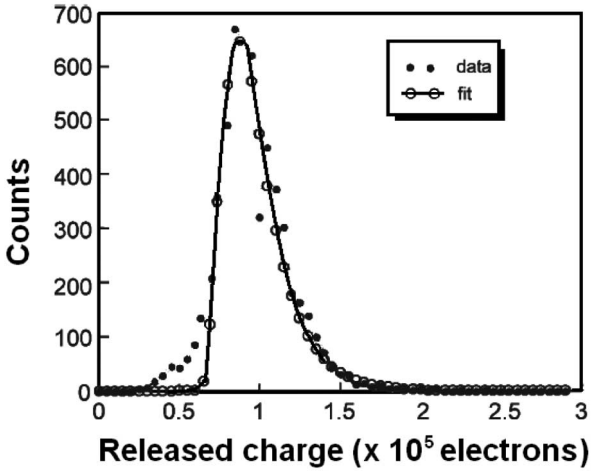

Fig. 4. – Histogram of the released charge from 60 MeV proton beam in a silicon strip.

channel. In the plot measured data (dots) is compared to the Landau fit (circles and line). The released charge mean value is equal to $8.7 \cdot 10^4$ electrons while the Monte Carlo prediction is $1.05 \cdot 10^5$ electrons. The discrepancy of 20% can be ascribed to the tolerance of integrated ASIC input capacitance values used in the calibration phase.

The YAG:Ce calorimeter was tested with protons at LNS, and at Loma Linda University Medical Center (LLUMC). In fig. 5 typical charge spectra at different energies are shown. The lower energies are obtained using PMMA slices to degrade the 60 MeV primary beam. The FWHM resolution at 60 MeV is 3.7%. The crystal response is linear (about 1% error) in the 30–60 MeV proton energy range. Tests performed at LLUMC show a good resolution also whit proton energy up to 200 MeV (1–2%). Moreover, using a tracker, we have verify that the crystal is homogeneous in the whole area.

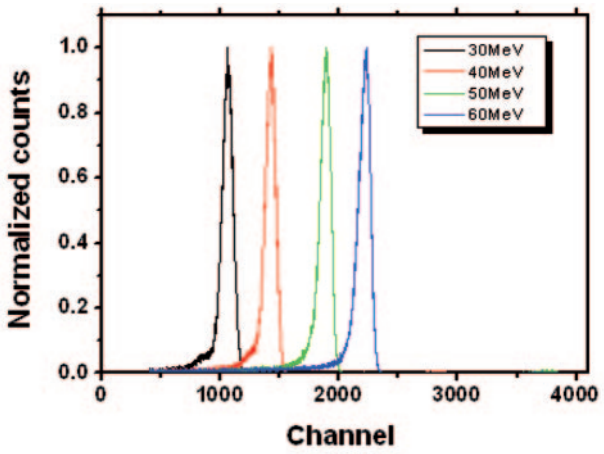

Fig. 5. – Charge spectrum obtained with different proton energy beam and YAG:Ce calorimeter.

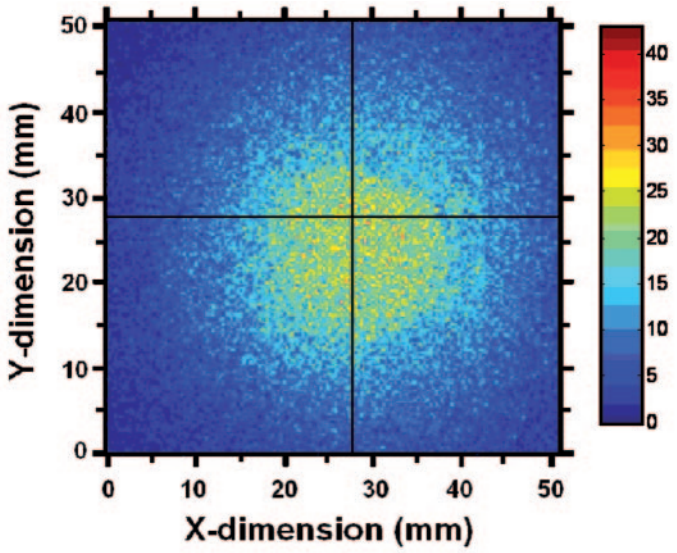

Fig. 6. – Counting map of the event triggered by the calorimeter with 60 MeV proton beam. The x-y coordinates correspond to the last x-y silicon plane near the calorimeter.

The test results of the complete apparatus, with the tracker and the calorimeter, are in advanced status of analysis. Figure 6 shows the map of the events triggered by the calorimeter in the alignment phase of the system. In order to plot this map, where the beam spot is evident, the x-y coordinates of the last silicon plane have been used. In the radiographic reconstruction it is necessary to apply to the data an algorithm, currently in review phase, that employs the calculus of the particle most likely path in the phantom.

5. – Conclusions

A system for pCR has been developed and the first test with proton beam has been performed. The apparatus includes a tracker based on Si microstrip detectors and a segmented YAG:Ce calorimeter. Previously, all the components had been manufactured and tested separately with β-source and with protons of various energies. Results of beam tests, performed at INFN-LNS with 1–50 kHz proton rate range, have been discussed in this paper. Finally, tests of the completed apparatus have been performed and have demonstrated the good performances of the data acquisition system. The data from various tracker modules and from the calorimeter have been correlated offline by using GEN tag, confirming that an unambiguous event building can be carried out. The image of the beam spot has been appreciated as shown in the previous section, the first phantom image has been acquired and the data analysis is in progress. The reconstruction algorithm is in the review phase and will be applied to the existing data. In order to demonstrate the functionality as radiography system, new tests need to use higher proton beam energies. For this reason, a beam test with 200 MeV protons at Essen WPC is scheduled by the end of 2011.

REFERENCES

[1] Miller D. W., *Med. Phys.*, **22** (1995) 1943.
[2] Amaldi U. *et al.*, *Rep. Prog. Phys.*, **68** (2005) 1861.
[3] Dosanjh M. *et al.*, *Nucl. Instrum. Methods A*, **571** (2007) 191.
[4] Schneider U. *et al.*, *Phys. Med. Biol.*, **41** (1996) 111.
[5] Zygmanski P. *et al.*, *Phys. Med. Biol.*, **45** (2000) 511.
[6] Cirrone G. A. P. *et al.*, *Nucl. Instrum. Methods A*, **576** (2007) 194.
[7] Schneider U. *et al.*, *Med. Phys.*, **21** (1994) 1657.
[8] Hanson K. M. *et al.*, *Phys. Med. Biol.*, **26** (1981) 965.
[9] Sipala V. *et al.*, *Nucl. Phys. B (Proc. Suppl.)*, **197** (2009) 39.
[10] Sipala V. *et al.*, *Nucl. Instrum. Methods A*, **612** (2010) 566.
[11] Menichelli D. *et al.*, *IEEE TNS*, Vol. **57**, No. 1, February 2010.
[12] Civinini C. *et al.*, *Nucl. Instrum. Methods A*, **623** (2010) 588.
[13] Williams D. C., *Phys. Med. Biol.*, **49** (2004) 2899.
[14] Talamonti C. *et al.*, *Nucl. Instrum. Methods A*, **612** (2010) 571.
[15] `www.crytur.com`.
[16] `http://sales.hamamatsu.com/assets/pdf/parts_S/s3204_etc_kpin1051e08.pdf`.
[17] Pullia A. *et al.*, *IEEE TNS*, Vol. **48**, No. 3 (2001).
[18] `www.strategic-test.com`.
[19] `http://www.policlinico.unict.it/Adroterapia/def.htm`.